ACS Catalysis

Article

A Pt/TiH2 catalyst for ionic hydrogenation via stored hydrides in the presence of gaseous H2

QiFan Wu, Chao Zhang, Masahiko Arai, Bin Michael Zhang, Ruhui Shi, Peixuan Wu, Zhuangqing Wang, Qiang Liu, Ke Liu, Weiwei Lin, Haiyang Cheng, and Fengyu Zhao

ACS Catal., **Just Accepted Manuscript** • DOI: 10.1021/acscatal.9b00917 • Publication Date (Web): 14 Jun 2019

A Pt/TiH_2 Catalyst for Ionic Hydrogenation via Stored Hydrides in the Presence of Gaseous H_2

Qifan Wu,[a,b,c] *Chao Zhang,*[*a,c] *Masahiko Arai,*[a,c] *Bin Zhang,*[a,b,c] *Ruhui Shi,*[a,b,c] *Peixuan Wu,*[a,b,c] *Zhuangqing Wang,*[a,b,c] *Qiang Liu,*[a,c] *Ke Liu,*[a,c] *Weiwei Lin,*[a,c] *Haiyang Cheng,*[a,c] *and Fengyu Zhao*[*a,c]

[a]State Key Laboratory of Electroanalytical Chemistry, Changchun Institute of Applied Chemistry, Chinese Academy of Sciences, Changchun 130022, PR China

[b]School of Applied Chemistry and Engineering, University of Science and Technology of China, Hefei, Anhui 230026, PR China

[c]Jilin Province Key Laboratory of Green Chemistry and Process, Changchun Institute of Applied Chemistry, Chinese Academy of Sciences, Changchun 130022, PR China

[*]Corresponding author, Tel: +86-431-85262410; Fax: +86-431-85262410;

E-mail address: czhang@ciac.ac.cn, zhaofy@ciac.ac.cn

ABSTRACT

A Pt/TiH_2 catalyst having hydrogen storage and release capability was investigated for selective hydrogenation of trans-cinnamaldehyde (CAL) to cinnamyl alcohol (COL) with gaseous dihydrogen. The catalytic behavior of this catalyst was significantly different from that of a reference Pt/TiO_2 catalyst with respect to the product selectivity and the hydrogenation mechanism. The Pt/TiH_2 catalyst showed a COL selectivity of 97% at a CAL conversion of 98%, which was ascribed to the function of Pt crystallite - support boundary layer that caused the preferential adsorption of CAL with its carbonyl group. Furthermore, the carbonyl group was hydrogenated by hydride species (H^+, H^-) supplied from the support and the hydride species consumed were compensated from gaseous dihydrogen; hydrogen atoms were formed by ordinary homolytic cleavage on Pt and then these hydrogen atoms moved onto the surface of TiH_2 and diffused into the bulk of the support, during which those simultaneously changed to hydride species (H^+, H^-) via electron transfer with titanium species and hydride vacancies therein. The surface and bulk diffusion of the hydrogen atoms from Pt to TiH_2 support should be dominant step rather than their addition to the carbonyl group of CAL (ordinary hydrogenation). That is, ionic hydrogenation occurs with Pt/TiH_2 in the presence of gaseous dihydrogen.

KEYWORDS: Hydrogenation, TiH_2, hydrogen storage materials, H-D exchange, heterolytic, trans-cinnamaldehyde

1. INTRODUCTION

Hydrogenation reactions are a major contributor to current chemical processes (6%), for the upgrading of crude oils and the production of commodity, fine chemicals, pharmaceuticals, jet fuel and so on.[1] Gaseous hydrogen is a general reducing agent in practical hydrogenation processes and its activation can occur through homolytic or heterolytic cleavage. Homolytic cleavage of H_2 always takes place easily over a metal catalyst, which has been extensively studied and used in hydrogenation reactions.[2] Heterolytic activation of H_2 is highly favored and desired for the selective hydrogenation of polar groups (for example, carbonyl groups) than non-polar groups (for example, carbon-carbon multiple bonds) and in some semi-hydrogenation reactions.[3] Heterolytic cleavage of H_2 has been achieved with homogeneous catalysts such as Frustrated Lewis Pairs; however, it is still a big challenge for heterogeneous catalysts[1e, 3b, 4]. Although heterolytic activation of H_2 requires more energy (ΔH_0 = 17.35 eV) to produce H^+ and H^-, as compared to the homolytic activation of H_2 (ΔH_0 = 4.5 eV) to produce $2H\cdot$, it is not impossible with some heterogeneous catalysts.[4c, 4d, 5] Previous studies have obtained some interesting

and useful information on heterolytic cleavage of H_2 on metal oxide catalysts.[3a, 6] However, there are still important, open questions worthy of further investigation that have been attracting interests of researchers in the related fields: How are heterolytic hydrogen species generated? What are exact active centers? Does the heterolytic hydrogenation occur with conventional catalysts? It is of scientific significance, therefore, to explore new heterogeneous catalysts that can efficiently generate heterolytically cleaved hydrogen and promote the desired selective hydrogenation and to investigate reaction mechanisms of these processes/steps.

In the past few decades, hydrogen storage materials have received much attention due to the green and safe generation of hydrogen.[7] Hydrogen storage materials show unique properties of storage and release of hydrogen. In most cases, the stored hydrogen is not electronically neutral but negatively charged and the released hydrogen could be highly active. Hydrogenation reactions would occur in the absence of additional hydrogen sources if the stored hydrogen could be released and available for the reactions, for which the effective hydrogen storage and reusability of these materials should carefully be considered. It is interesting to know and examine difference in the catalytic actions between hydrogen species (hydrogen radicals) formed via homolysis of dihydrogen and hydrogen species (charged hydrogen

species) released from the hydrogen storage materials. Unfortunately, there are very few reports concerned with such an important and interesting issue of heterogeneous catalysis in the literature.

Considering the above-mentioned circumstances and taking notice of its hydrogen storage properties, the authors have selected a material of TiH_2 as a catalyst support and studied the activity of TiH_2 - supported Pt catalysts for a model reaction of liquid-phase selective hydrogenation of *trans*-cinnamaldehyde (CAL) to cinnamyl alcohol (COL). TiH_2 is one of interesting hydrogen storage materials, which can uptake hydrogen of more than 4% in weight (about 20 mmol dihydrogen per 1 g). In the present work, various Pt/TiH_2 catalysts were prepared under different reduction conditions and tested for the selective hydrogenation of CAL. It should be noted here that a Pt/TiH_2 catalyst reduced at a medium temperature (150 ºC) is highly selective to the hydrogenation of C=O bond with an excellent selectivity of 97% to COL, in contrast to low COL selectivity values with other Pt/TiH_2 catalysts reduced at higher temperatures and a reference Pt/TiO_2 catalyst. In order to examine the functions of TiH_2 and Pt, the structures and properties of the catalysts prepared were examined by different methods including TPR, TPD, XPS, in-situ DRIFT, TEM, and GC-MS. Furthermore, isotope experiments were also conducted, in which CAL hydrogenation

was tested with D_2 over Pt/TiH_2 catalysts containing no and some amount of D species included by reduction in D_2. On the basis of those reaction and characterization results, it is confirmed that 1) the perimeter of Pt nanoparticles and TiH_2 support is the active center; 2) the stored hydrogen species contribute to the heterolytic hydrogenation with H^+ and H^-; 3) the TiH_2 support plays a role like "Frustrated Lewis Pair" to stabilize and separate the H^+ and H^-. To our best knowledge, it is the first report on heterolytic hydrogenation reactions over supported Pt catalysts with hydrogen storage TiH_2 as a carrier. It is expected that this study can provide useful knowledge for the design of a new type of active supported metal catalysts featuring the hydrogen storage capability and the production of heterolytic hydrogen species for selective hydrogenation and other reactions.

2. EXPERIMENTTAL

2.1 Materials. Commercially available reagents, *trans*-cinnamaldehyde (CAL) (Beijing JK chemical; >99.0%), $H_2PtCl_6 \cdot 6H_2O$ (Jilin Haodi; ≥ 99.9%), TiH_2 (Aladdin, >99.0%), titanium (IV) oxide, TiO_2 (P25) (Acros), isopropanol, toluene and cyclohexane (Beijing chemicals; ≥ 99.9 %) were used as received.

2.2 Catalysts Preparation. Onto TiH_2 supports, Pt was loaded in different contents of Pt (0.1, 1.0 and 5.0 wt.-%) by incipient wetness method. $H_2PtCl_6 \cdot 6H_2O$ was

dissolved in water and then TiH_2 support was added to form a slurry mixture. The slurry was dried at 50 ºC in a water bath while stirring and then kept at 50 ºC in an oven overnight. Prior to usage, the Pt-loaded samples were reduced under pure H_2 flow at temperatures, T, of 150 ºC, 350 ºC and 450 ºC for 2 h. The catalysts are referred to as (Pt/TiH_2)-TH_2 in the following. To vary the structural properties of support, the following treatments were made for parent TiH_2 sample. It was treated with H_2 at 150 ºC or 450 ºC for 2 h and then with N_2 at decreasing temperatures for 0.5 h. The treated support is referred to as TiH_2-150H_2 or TiH_2-450H_2. For comparison, a commercial TiO_2 (P25) was also used as a support for Pt.

2.3 Catalyst Characterization. The TiH_2 supports and Pt loaded catalysts were characterized by the following methods. X-ray photoelectron spectroscopy (XPS) measurements without sputtering were carried on VG Microtech 3000 Multilab and those with sputtering on ESCALAB 250Xi, ThermoScientific, in which the sample was sputtered by Ar to a depth of 3 nm. X-ray powder diffraction (XRD) measurements were carried on a Bruker D8 ADVANCE diffractometer, using Cu Kα radiation (k = 0.154 nm). Transmission electron microscopy (TEM) images were collected on a JEOL JEM-2010 operated at an accelerating voltage of 200 kV. The size and metal dispersion of Pt nanoparticles were also examined by CO pulse

chemisorption at 50 ºC with a pulse of CO (10%) in He on Micromeritics AutoChem II 2920. Temperature programmed reduction (TPR) profiles were measured on Micromeritics AutoChem II 2920. For TPR, a sample (100 mg) was treated with Ar at 100 ºC for 0.5 h to remove H_2O adsorbed and cooled to 50 ºC. Then, the sample was heated at 5 ºC/min to 900 ºC in a stream of H_2 (10%) in Ar mixture at a flow rate of 50 mL/min. The amount of H_2 consumed was measured by a thermal conductivity detector (TCD). H_2 release profiles were collected on Micromeritics AutoChem II 2920. A sample (100 mg) was reduced with H_2 (10%) in Ar at a certain temperature for 0.5 h and cooled to 50 ºC. Then, the sample was heated at 50 ºC/min to 900 ºC in a stream of Ar at a flow rate of 50 mL/min and the amounts of species evolved were measure by TCD. H_2 release profiles was also made on QIC-20, Hiden, UK, with a mass spectrometer using a sample of 50 mg, which was pretreated in the same manner as mentioned above. The adsorption of the substrate, CAL, was examined by in situ diffuse reflectance infrared Fourier transform spectroscopy (DRIFT) on Thermo Scientific Nicolet 6700 Fourier transform infrared spectroscopy. A catalyst sample was reduced at 150 ºC for 30 min in a DRIFT cell with 10% H_2/Ar mixture (30 mL/min) and then cooled to 30 ºC. The cell was purged with He (30 mL/min) for 30 min and the background spectrum was recorded. After 40 μL substrate (0.5 M in

isopropanol) was introduced to the sample, the temperature of the cell was raised to 150 ºC slowly while passing He (30 mL/min). The spectrum was recorded at 150 ºC every 30 min until all the physically adsorbed species were removed.

2.4 Selective Hydrogenation. The catalytic performance of Pt on TiH_2 supports was tested for the selective hydrogenation of CAL using a 50 mL stainless steel autoclave with an inner Teflon coating. For a typical catalytic reaction, 1.0 mmol CAL and 50 mg catalyst were mixed in 5 mL of an organic solvent in the reactor. It was purged with 1 MPa H_2 three times and then sealed. The reaction was conducted at 4 MPa H_2 and at 100 ºC. The products were analyzed by a gas chromatograph (Shimadzu, 2010) equipped with a capillary column (Restek-50 30 m × 0.25 mm × 0.25 μm) and a flame ionization detector (FID). Conversion was determined by dividing the amount of CAL consumed by the initial amount of CAL; product selectivity was calculated by dividing the amount of a certain product by the amount of CAL consumed. Site-time-yield was calculated by dividing the amount of a certain product by the amount of exposed Pt atoms determined by CO pulse chemisorption and reaction time. The recycling test was performed as following: The reacted catalyst was separated by centrifugations and washed three times by isopropanol. The catalyst

was then used in the next recycling test, and the reaction conditions were the same each time.

3. RESULTS AND DISCUSSION

The catalytic performance of Pt/TiH_2 materials was examined using a model reaction of selective hydrogenation of trans-cinnamaldehyde (CAL) to cinnamly alcohol (COL) (Scheme 1), in which COL and hydrocinnamaldehyde (HCAL) are produced via hydrogenation of C=O and C=C, respectively, with hydrocinnamyl alcohol (HCOL) as the final hydrogenation product. In some cases, condensation products of organic solvents and CAL are formed. The performance of Pt/TiH_2 catalysts was tested in CAL hydrogenation with H_2. Further, the CAL hydrogenation was also conducted with D_2 over Pt/TiH_2 catalysts to examine their catalytic features. Then the physicochemical properties of these catalysts were examined by several techniques to discuss the catalysis of selective CAL hydrogenation to COL on a new kind of Pt/TiH_2 catalysts.

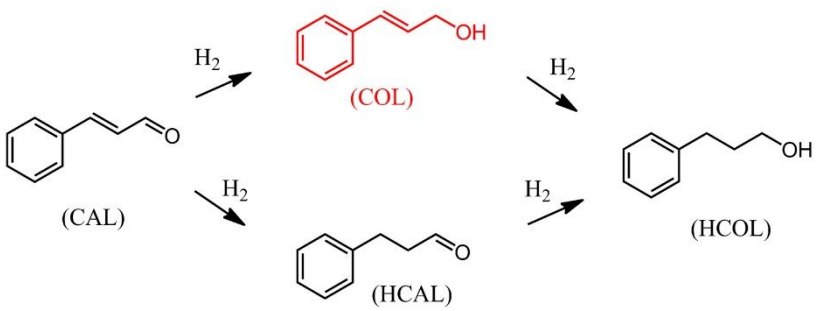

Scheme 1. Reaction pathways for hydrogenation of CAL.

3.1 Selective Hydrogenation with H_2. Table 1 shows the results of CAL hydrogenation with TiH_2 and Pt/TiH_2 samples. The supports alone, untreated and treated in H_2 at 150 ºC, were marginally active and the COL selectivity was small with appreciable amounts of other condensation products from CAL and the solvent, isopropanol (entries 1, 2). The loading of Pt in 1.0 wt.-% to TiH_2 increased the conversion to 67% from 6% in 3 h and the COL selectivity to 52% from 34% but the condensation products were also produced (entry 3). When the Pt/TiH_2 sample was reduced by H_2 at 150 ºC, the conversion was further increased to 83% and, more interestingly, a high COL selectivity of 97% was obtained with even smaller amounts of HCAL, HCOL, and the condensation products (entry 4). When the reaction was conducted in N_2 instead of H_2, only a small amount of CAL was consumed and a (relatively) large amount of byproducts was detected. That is, almost no hydrogenation reaction occurred in N_2 (entries 5, 6). The time profiles of total conversion and product selectivity with the highly active (1%Pt/TiH_2)-150H_2 catalyst is given in Supporting Information (SI, Figure S1).

The influence of Pt loading on the performance of Pt/TiH_2 catalyst was examined with 0.1, 1.0, and 5.0 wt.-% Pt samples reduced at 150 ºC. As shown in Table S1, the CAL conversion was found to decrease with the Pt loading, in particular, with 5.0

wt.-% Pt. However, the high COL selectivity remained unchanged, being > 90% for those catalysts examined.

Table 1. Results of CAL hydrogenation over different catalysts.

Entry	Catalyst	Time (h)	Conversion (%)	Selectivity (%)			
				COL	HCAL	HCOL	Others[a]
1	TiH_2	3	6	34	5	7	54
2	TiH_2-150H_2	6	3	22	8	5	65
3	1.0%Pt/TiH_2	3	67	52	7	6	35
4	(1.0%Pt/TiH_2)-150H_2	3	83	97	1	1	1
5	TiH_2[b]	3	3	2	1	5	92
6	(1.0%Pt/TiH_2)-150H_2[b]	3	3	1	0	7	92

Reaction conditions: 50 mg catalyst, 1 mmol CAL, 5 mL isopropanol, 100 ºC, 4 MPa H_2.

a. Products from the condensation of CAL and isopropanol.

b. 4 MPa N_2 was used instead of H_2.

Table 2 shows the results of 1.0 wt.-% Pt/TiH_2 reduced at different temperatures. The catalytic activity markedly decreased with an increase in the reduction temperature; the CAL conversion was 98% in 4 h, 11% in 6 h, and 18% in 24 h for the catalysts reduced at 150 ºC, 350 ºC, and 450 ºC, respectively (entries 1-3). The catalyst reduced at 350 ºC still maintained a high COL selectivity of 88% but that at 450 ºC had a lower selectivity of 78% with the formation of condensation products in

20%. In addition, the influence of TiH_2 pretreatment with H_2 was examined, in which the reduction of Pt was conducted at 150 ºC. The TiH_2 pretreatment at a higher temperature of 450 ºC decreased the CAL conversion but little altered the high COL selectivity (entry 5). All the Pt/TiH_2 catalysts reduced at 150, 350 and 450 ºC showed large C=O hydrogenation selectivity values. There is a difference in the COL selectivity between the catalysts reduced at 350 ºC and 450 ºC (entries 2, 3), which is due to the production of more condensation products for the latter catalyst. The sizes of supported Pt particles were different, being 2.0, 4.4, 5.1 nm for those reduced at 150, 350 and 450 ºC, respectively (Table S2), and there were only slight differences in the XPS Pt 4f binding energy (Figure S2). Therefore, the surface properties of Pt particles should not be crucial for the high selective hydrogenation of C=O bond of CAL over the Pt/TiH_2 catalysts. For comparison, the activity of 1.0 wt.-% Pt/TiO_2 (P25) was tested under the same conditions. The catalyst reduced at 150 ºC was more active than the Pt/TiH_2 reduced at the same temperature (Table 1 entry 4, Table 2 entry 6) but it was less selective to the COL formation (22% selectivity) with a larger amount of condensation products. When the reduction was conducted at a higher temperature of 450 ºC, the Pt/TiO_2 catalyst became more selective to the hydrogenation of C=O giving a COL selectivity of 77%, which was still smaller than

97% of the Pt/TiH_2 catalyst. The relatively high COL selectivity of the 450 ºC - reduced catalyst can be interpreted by strong metal - support interaction (SMSI) via electron transfer from the support to the Pt particles. Such a (partially) negatively charged Pt surface would facilitate the adsorption of C=O bond rather than C=C bond, promoting the selective hydrogenation of the former.[8] For the two Pt catalysts on TiH_2 and TiO_2 supports reduced at a lower temperature of 150 ºC, in which the sizes of Pt particles were comparable (about 2 nm) as seen in Figure S3, the configuration of CAL adsorption should be different between the two catalysts.

Table 2. Results of hydrogenation of CAL over Pt/TiH_2 and Pt/TiO_2 catalysts reduced at different temperatures.

Entry	Catalyst	Time (h)	Conversion (%)	Selectivity (%)			
				COL	HCAL	HCOL	Others[a]
1	(1.0%Pt/TiH_2)-150H_2	4	98	97	0	1	2
2	(1.0%Pt/TiH_2)-350H_2	6	11	88	4	0	8
3	(1.0%Pt/TiH_2)-450H_2	24	18	78	2	0	20
4	(1.0%Pt/(TiH_2-150H_2))-150H_2	4	99	97	0	3	0
5	(1.0%Pt/(TiH_2-450H_2))-150H_2	4	67	94	3	2	1
6	(1.0%Pt/TiO_2)-150H_2	3	93	22	6	6	66
7	(1.0%Pt/TiO_2)-450H_2	3	95	77	2	21	0

Reaction conditions: 50 mg catalyst, 1 mmol CAL, 5 mL isopropanol, 100 ºC, 4 MPa H_2.

a. Products from the condensation of CAL and isopropanol.

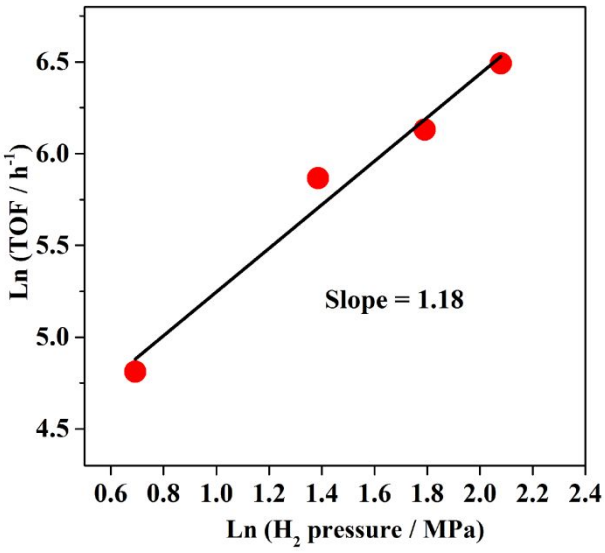

Figure 1. H_2 pressure dependence in hydrogenation of CAL over (Pt/TiH_2)-150H_2. Reaction conditions: 25 mg catalyst, 1mmol CAL, 5 mL isopropanol, 100 ºC, 2, 4, 6 and 8 MPa H_2. The TOF was calculated at the conversion values of 6%, 8%, 8% and 8%, at different H_2 pressures.

Further, the influence of H_2 pressure was examined for CAL hydrogenation using the most active catalyst of (1.0%Pt/TiH_2)-150H_2. Figure 1 shows the results collected at H_2 pressures of 2 - 8 MPa. A linear relationship was found to exist in the logarithmic plot of turnover frequency (TOF) against H_2 pressure and, interestingly, its slope was 1.18. This value was significantly different from the result with the reference catalyst of (1.0%Pt/TiO_2)-150H_2, for which a slope of 0.61 was observed (Figure S4) under the same reaction conditions. As indicated by Tomishige et al. in

the hydrogenation of crotonaldehyde,[3a] dicarboxylic acids[9] and ethers[10], a reaction order of around 1 means that hydride (H^-) is more likely involved in the rate-determining step. Thus, Figure 1 suggests that the present hydrogenation of CAL over Pt/TiH_2 catalyst is unlikely to occur via ordinary reaction processes that H_2 is dissociatively adsorbed on Pt followed by the addition of H species to the unsaturated bonds of the adsorbed CAL molecules. Detailed mechanisms of the catalysis over the Pt/TiH_2 will be discussed later.

3.2 Selective Hydrogenation with D_2. To obtain further information about the catalysis of a new type of catalyst of Pt/TiH_2, D_2 was used, instead of H_2, for the CAL hydrogenation and the catalyst reduction (Table 3 and Table S3). The average sizes of Pt crystallites in the catalysts reduced in H_2 and D_2 were observed to be comparable (both were about 2.0 nm, Table S2). The two catalysts showed comparable initial TOF values in H_2, but quite different ones in D_2 (Table S3). Under the reaction conditions used, the GC-MS analysis detected the formation of four kinds of COL molecules different in the molecular weight (MW = 134, 135, or 136), indicating COL formed via the addition of two H atoms to CAL, one D atom and one H atom, or two D atoms, respectively. Noteworthy, a relative higher conversion is necessary for the accurate analysis of the molecular weight of COL, and it was impossible to

estimate the distribution of COL molecules (MW = 134, 135, 136) by the present analysis. Table 3 gives important and interesting pieces of information: (1) the COL selectivity is high in D_2 as well as in H_2 (entries 1 - 5), (2) COL molecule including D atom is formed in H_2 even when the catalyst is pre-reduced in D_2 (entry 3), similar to the reaction in D_2 with the catalyst pre-reduced in H_2 (entry 2), (3) the rate of COL formation (STY_{COL} and TOF) is smaller for the reaction in D_2 with the catalyst reduced in H_2 (entry 2) compared with the other reactions. The STY_{COL}(TOF) values are comparable for the reactions with the (Pt/TiH_2)-150H_2 in H_2 (entry 1) and those with the (Pt/TiH_2)-150D_2 in H_2 (entry 3) and in D_2 (entry 4). Note again that the D species in the support were included in the COL molecules and the influence of gaseous D_2 appeared on the rate of reaction only in the case of the catalyst reduced in H_2, in which D species are absent in the support. Those results indicate that the present CAL hydrogenation over the Pt/TiH_2 catalysts occurs via ionic hydrogenation. Besides, the diffusion of H/D species in TiH_2 is crucial for the reaction rate. In addition, an additional interesting fact was observed: (4) when cyclohexane was used as a solvent instead of isopropanol, COL (MW = 136, product D) and COL (MW = 135, product C) were formed but these were not detected in the reactions in

isopropanol. It is probable that there occurred fast H-D exchange between isopropanol and COL molecules, resulting in no COL products C and D detected in isopropanol.

Table 3. Results of CAL hydrogenation with 1%Pt/TiH_2 catalysts using H_2 and D_2 for CAL hydrogenation and catalyst reduction.

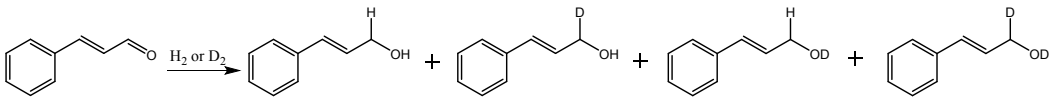

A (MW = 134) **B** (MW = 135) **C** (MW = 135) **D** (MW = 136)

Entry	Catalyst	Conversion (%)	Time (h)	Reaction gas	COL[a] (%)	A[b]	B[b]	C[b]	D[b]	STY_{COL}[c] (h^{-1})
1	(1.0%Pt/TiH_2) -150H_2	49	1	H_2	93.3	○	X	X	X	343
2		68	4	D_2	86.6	○	○	X	X	110
3	(1.0%Pt/TiH_2) -150D_2	30	0.5	H_2	88.7	○	○	X	X	399
4		55	1	D_2	95.2	○	○	X	X	392
5[d]		31	2	D_2	96.5	○	○	○	○	112

Reaction conditions: 50 mg catalyst, 1 mmol CAL, 5 mL isopropanol, 100 ºC, 4 MPa H_2 or D_2.

a. Total COL selectivity.

b. "○" and "X" represent that the product was and was not detected, respectively.

c. STY = mole of COL produced per mole of exposed Pt atoms per 1 h. (The amount of exposed Pt atoms was determined by CO pulse chemisorption)

d. Cyclohexane was used instead of isopropanol. Reaction conditions: 50 mg catalyst, 1 mmol CAL, 10 mL cyclohexane, 100 ºC, 4 MPa D_2.

3.3 Catalyst Characterization. The structure of TiH_2 was examined by XRD. The XRD patterns of TiH_2 treated in H_2 at different temperatures of 150, 350, 450 ºC are given in SI (Figure S5). The diffraction peaks at 2θ = 35.0, 40.6, 58.8, 70.2 and 73.8º are respectively indexed to the (111), (200), (220), (311), and (222) planes of cubic TiH_2[11] (JCPDF:25-0982). The structure did not change by the treatment in H_2 at 350 ºC or below but that at a higher temperature of 450 ºC caused the phase change to some extent from cubic ($TiH_{1.92}$) to tetragonal phase ($TiH_{1.92}$). The XRD patterns for 1.0 wt.-% Pt loaded samples were identical with those of the supports alone, indicating that the support structure did not change on the loading of Pt by incipient wetness and the subsequent reduction (Figure S6). Pt was dispersed on the supports in the form of small nanoparticles with very weak XRD diffraction peaks.

Then, the H_2 reduction behavior of as-prepared samples with and without Pt was examined. Figure 2 shows two H_2 consumption peaks at 450 ºC and 576 ºC for both TiH_2 and 1.0 wt.-% Pt/TiH_2 samples. The former and latter H_2 consumption peaks should correspond to the hydrogen storage by β-TiH_x and α-Ti phases, respectively.[12] Either the amount of H_2 consumed in the low-temperature region or that in the high-temperature region was the same between the two samples. It is interesting to note, therefore, that no H_2 consumption due to the reduction of Pt precursors to Pt was

observed. The Pt reduction should be already completed during the catalyst preparation, for which the support is likely to contribute to the reduction.

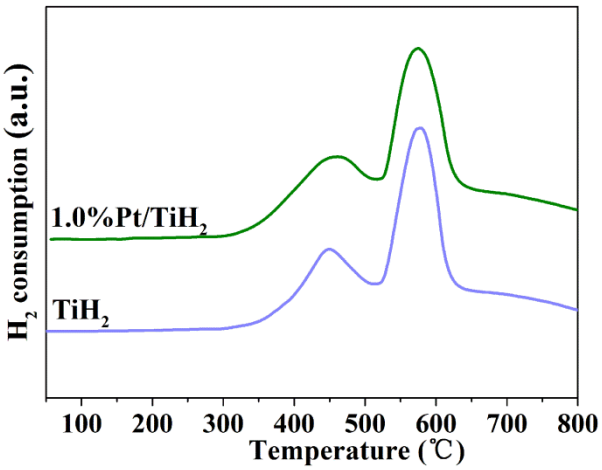

Figure 2. H_2-TPR profiles of Pt/TiH_2 catalyst and TiH_2 support.

In addition, the thermal behavior of TiH_2 and Pt/TiH_2 samples reduced at different temperatures was examined, in which a sample was heated in Ar at 50 mL/min and at a heating rate of 10 ºC/min and the amount of H_2 released was measured. Figure 3 shows that H_2 is released at two temperature regions, 350 - 450 ºC and 450 - 550 ºC, which should correspond to the dehydrogenation of TiH_2 to β-TiH_x phase and β-TiH_x to α-Ti phase, respectively. That is, hydrogen species stored in the support are releasing out under the heat treatment. It should be noted that the hydrogen release in the low-temperature region moved to much lower temperature in the presence of Pt for the catalyst reduced at 150 ºC; the metal facilitates the release of hydrogen from

the support.[13] For the samples reduced at higher temperature (350 and 450 ºC), however, such an effect of Pt was not observed.

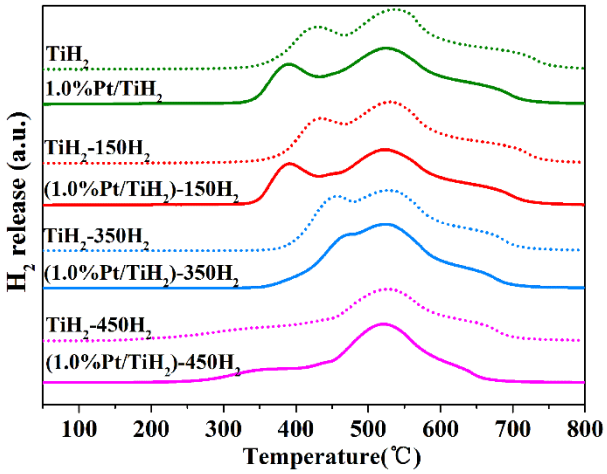

Figure 3. H_2 release profiles of Pt/TiH_2 catalysts and TiH_2 supports reduced at different temperatures during heating in an inert atmosphere measured by TCD.

The thermal gas releasing behavior was also examined for 1.0 wt.-% Pt loaded catalyst that was reduced in H_2 and then used in CAL hydrogenation in D_2. Figure 4 gives the results of fresh and used catalysts, in which H_2, H_2O, and/or D_2O were detected. The release of H_2 was observed to occur in two temperature regions, which were maximized at 430 ºC and 510 ºC. The former is due to the hydrogen release from β-TiH_x while the latter from α-Ti, as described above.[12] For H_2O, it was released in a small quantity at about 110 ºC, due to desorption of adsorbed water, and in a larger quantity at higher temperatures with two peaks at about 435 ºC and 515 ºC. The H_2O releasing at high temperatures should be related to the decomposition of TiO_xH_y

composite on the surface of the TiH_2 support. Note that although the Pt/TiH_2 sample did not contain D species, two D_2O peaks (merged) at around 90 ºC and 350 ºC were also detected after the hydrogenation in D_2, during which D species were therefore taken in the catalyst (support). For the catalyst used in the CAL hydrogenation in H_2, H species are also likely to be included. These results indicate that the storage and release of hydrogen species occur for the Pt/TiH_2 catalyst; the results of Figure 4 demonstrate that hydrogen species move between the gas (H_2, D_2) and solid (catalyst) phases. From the results of CAL hydrogenation using D_2 and H_2 (Table 3 and Table S3) and catalyst characterization (Figures 3 and 4), it can be assumed that, for the present three-phase reaction system, the transfer of hydrogen species takes place between the gas and liquid (solvent) phases (dissolution) and between the liquid and solid (catalyst) phases (storage and release). This hydrogen transfer will further be discussed later.

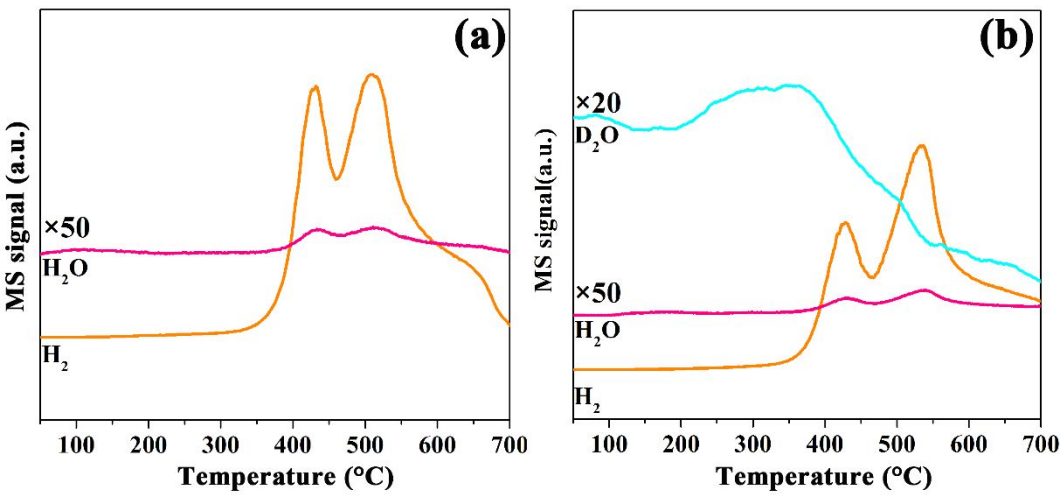

Figure 4. H_2, H_2O and D_2O release from (1%Pt/TiH_2)-150H_2: (a) fresh and (b) used in CAL hydrogenation in D_2 during heating in an inert atmosphere measured by MS.

The surface of Pt/TiH_2 was further examined by XPS with respect to the chemical state of Ti and O species. Figure S7 shows the results of XPS Ti 2p of the TiH_2 support and a series of Pt/TiH_2 catalysts. Various Ti species such as Ti^{2+}, Ti^{3+}, and Ti^{4+} were detected; the peaks at 455, 457, 458 and 458.8 eV are attributable to the Ti^{2+}, Ti^{3+}, Ti_3O_5 and Ti^{4+}, respectively.[11c, 14] Ti^{4+} species were dominant on Pt/TiH_2 (Figure S7b) surface and no Ti^{2+} was detected. When the sample was Ar sputtered by a depth of 3 nm, the relative amounts of Ti^{3+} and Ti_3O_5 increased, meaning that the chemical state of Ti species was quite different between the surface thin layer and the inner bulk phase, as shown in Figure S7d.[14b] Figure 5 gives the results of XPS O 1s, indicating the presence of three types of O species. It is assumed that one is related to the oxygen in Ti-O-Ti lattice (labeled as type A), one to either that near defect sites or Ti-OH (labeled as type B), and the other to chemically adsorbed oxygen-containing species (such as H_2O, labeled as type C).[14a] Note that the percentage of the "type B" O species (19%) was larger for Pt/TiH_2 catalysts, as compared with the reference Pt/TiO_2 catalyst (9%).

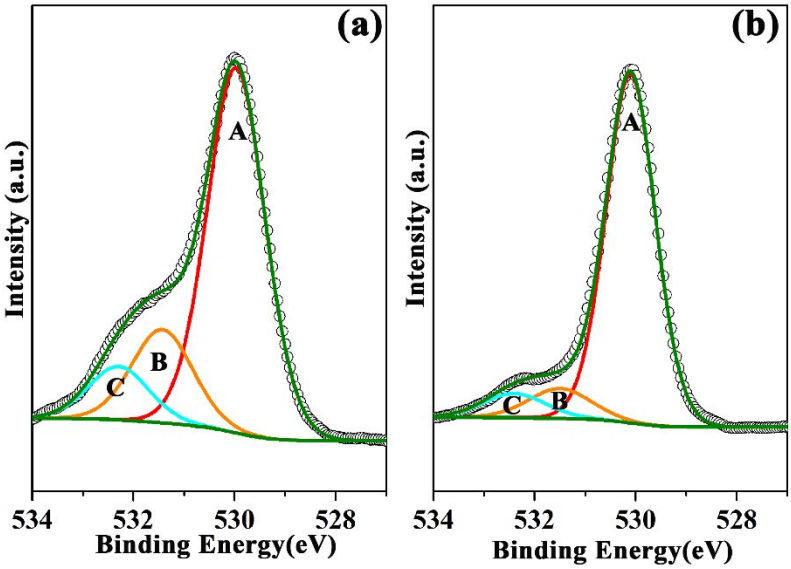

Figure 5. O1s XPS profiles of (1% Pt/TiH_2)-150H_2 (a) and (1%Pt/TiO_2)-150H_2 (b).

Finally, the adsorption of CAL substrate on TiH_2 alone and the most active catalyst of (1.0% Pt/TiH_2)-150H_2 was examined by in-situ DRIFT measurements. Figure 6 gives the DRIFT spectra collected (the assignment of absorption bands observed are given in Table S4). The absorption band at 1673 cm^{-1} can be indexed to stretching vibration of C=O group adsorbed physically on the samples, which was detected for all the four samples before the treatment with He. When the supports were treated by He gas at 150 ºC for 200 min, the absorption band at 1673 cm^{-1} almost disappeared for TiO_2 (P25) but two absorption bands remained at 1647 cm^{-1} and 1614 cm^{-1} for TiH_2, which were due to chemisorption of C=O and C=C bonds, respectively, and the latter was stronger than the former. Namely, the support of TiH_2 itself is likely to adsorb CAL molecules strongly in contrast to TiO_2. On the treatment with He at a

higher temperature of 250 ºC, the two chemical absorption bands disappeared over TiH_2, indicating all the CAL molecules were removed from the TiH_2. When Pt was loaded onto TiO_2, the absorption bands in the range of 1700 - 1600 cm^{-1} did not change significantly on the He treatment; from the presence of the chemisorption bands due to C=O and C=C groups, CAL was adsorbed with its C=C and C=O groups. For the He treated (Pt/TiH_2)-150H_2 catalyst, however, the absorption band at 1614 cm^{-1} was observed but not that at 1647 cm^{-1}. Those results indicate interesting differences in the adsorption of the substrate CAL between Pt/TiH_2 and TiH_2 and between Pt/TiH_2 and Pt/TiO_2 catalysts. For Pt/TiH_2, the coexistence of TiH_2 and Pt crystallites is significant for the CAL adsorption and should produce adsorption sites for CAL molecules at TiH_2 - Pt crystallite boundary. Probably, the adsorption of CAL occurs with its C=O group on the boundary (discussed later) and the unique adsorption is so strong (C=O bond becomes weakened) that the absorption band due to C=O cannot be detected. When the treatment with He was conducted at a higher temperature of 250 ºC, two absorption bands were again observed at 1647 cm^{-1} and 1614 cm^{-1} (Figure 6b). This should result from a change of the unique adsorption of CAL on the TiH_2 - Pt crystallite boundary at higher temperature.

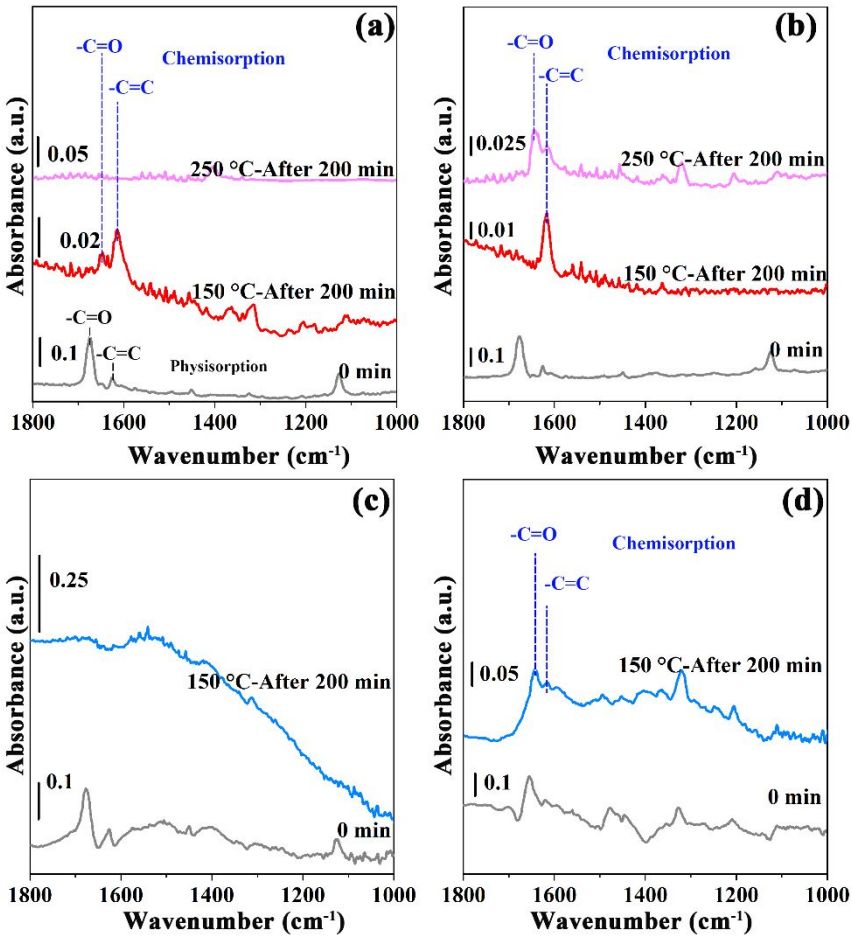

Figure 6. In-situ DRIFT absorption spectra of CAL over TiH_2 (a), (1.0%Pt/TiH_2)-150H_2 (b), TiO_2 (c), and (1.0%Pt/TiO_2)-150H_2 (d) before and after the treatment with He at 150 ºC. For (a) and (b), the data after the He treatment at 250 ºC is also presented.

3.4 Mechanism Consideration. As reported previously, various Ti species such as TiO_2, Ti_2O_3, TiO, Ti, etc. can exist on the surface of TiH_2.[14] Besides, oxyhydrides of TiO_xH_y could form on heating, and some of them had the same crystal structure and lattice parameters as TiH_2.[15] On the basis of the above-mentioned characterization

results, the TiH_2 support should be in the structure of a thin layer of TiO_xH_y covering the bulk TiH_2 as illustrated in Figure 7. The TiO_xH_y layer should be formed on the surface of TiH_2 during reduction at 150 ºC, in which various types of Ti species coexisted. When Pt was loaded onto such a support and reduced, it was dispersed in the form of nanoparticles of about 2 nm in size. When the reduced Pt/TiH_2 catalyst is exposed to gaseous H_2, hydrogen may be stored by the support; ordinary homolytic cleavage of H_2 takes place over the surface of Pt crystallites (Eq. 1). Then, resulting H species spillover on the TiO_xH_y surface via electron transfer with $Ti^{\delta+}$ and $Ti^{(\delta+1)+}$ species (Eq. 2 - 4). At the same time, the H species can also penetrate into the vacancy of TiH_2 lattices and be stored thereby in the form of H^-. Once H enters into TiH_2 lattice, it will form an H^- and an H vacancy with positive charge (V_H^+)[16] (Eq. 5). Both H^+ and H^- in the support have migration characteristics: The H^+ can spillover on and diffuse within the TiO_xH_y layer and the H^- can diffuse in the TiH_2 by contact with adjacent V_H^+, regenerating H (Eq. 6, 7). Also, the H^- can migrate to the surface of TiO_xH_y layer.

On Pt:

$$H_2 \rightarrow 2H \qquad (1)$$

On/within thin TiO_xH_y layer:

$H + Ti^{(\delta+1)+} \rightarrow H^+ + Ti^{\delta+}$ (2)

$Ti^{\delta+} \rightarrow Ti^{(\delta+1)+} + e^-$ (3)

$H^+ + e^- \rightarrow H$ (4)

Within bulk TiH_2:

$TiH_2 + H \rightarrow TiH_2(H^-) + V_H^+$ (5)

$TiH_2(H^-) \rightarrow TiH_2 + H^-$ (6)

$H^- + V_H^+ \rightarrow H$ (7)

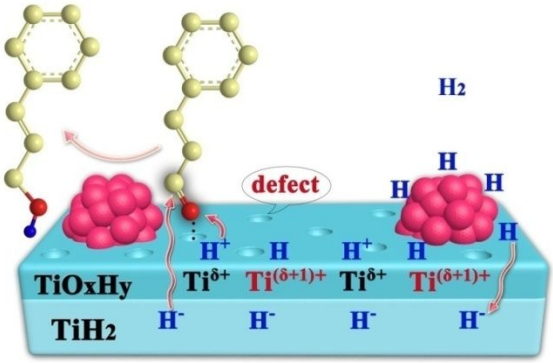

Figure 7. Possible reaction mechanism of hydrogenation of CAL over (Pt/TiH_2)-$150H_2$ catalyst. This is a simplified illustration: H^+ and H^- species are formed and stored in the thin TiO_xH_y layer and the TiH_2 bulk, respectively. H^+ and H^- will attack O and C atoms of the carbonyl group of CAL adsorbed on the Pt crystallite - support boundary.

The FTIR results suggest that CAL molecule is adsorbed on the boundary of TiH_2 support and Pt particles with its C=O bond (Figure 6). The surface of TiH_2 exposes the type B oxygen, oxygen species close to defects (oxygen vacancy) and of Ti-OH, as indicated by XPS (Figure 5). We believe that oxygen-free defect sites and/or Ti-OH sites serve as sites for the adsorption of the substrate molecule; O atom of a CAL molecule interacts with the defect site or H atom, which causes the CAL adsorption with its C=O bond preferentially than C=C bond. The strength of C=O bond is weak as demonstrated by FTIR and so the O atom of CAL should more likely interact with the defect sites than Ti-OH. The surface of Pt particles might interact with the C atom of CAL molecule and contribute the configuration of CAL molecules adsorbed on the catalyst. Thus, such preferential adsorption of CAL with its C=O bond is crucial for its selective hydrogenation to COL observed with the Pt/TiH_2 catalyst (Figure 7).

On the basis of the results of hydrogenation and catalyst characterization as above-mentioned, the present CAL hydrogenation over Pt/TiH_2 catalyst is likely to occur via unique processes different from ordinary ones through the dissociative adsorption (homolytic cleavage) of H_2 followed by the attack of the H atoms formed to a substrate adsorbed on a catalyst. In the present case, the hydrogen species to be

added to the substrate are supplied from the TiH_2 support, which are ionic species, H^+ and H^-, existing in the thin TiO_xH_y layer and TiH_2 bulk, respectively (Figure 7). Such a TiO_xH_y-covered TiH_2 structure will play a role like Frustrated Lewis Pair to separate and stabilize the H^+ and H^-species. The mobility and spillover of H^+ on metal oxides were extensively studied[17] and the H^- diffusion was also detected in the TiH_2-containing cell.[18] The selective hydrogenation of C=O bond depends on the controlled geometry of CAL adsorption; it is preferentially adsorbed with its C=O bond on Pt-support boundary as depicted in Figure 7. Due to such an adsorption mode, the C=O was weakened and polarized, which facilitated the attack of H^+ to the O atom and that of H^- to the C atom. Since the surface TiO_xH_y layer is very thin with a few nm in depth, H^- would be directly attacking the C atom of the aldehyde group of CAL.

TiH_2 can store hydrogen species in a maximum of 4 wt.-% and serve as a "hydrogen pool" for CAL hydrogenation (Figure 7). The loss of hydride species of the support consumed for the CAL hydrogenation should be compensated by gaseous H_2. A gaseous H_2 molecule is dissociatively adsorbed on Pt crystallites (as in ordinary hydrogenation) and the resulting H atoms diffuse to the support; then, two H species change to H^+ and H^- via electron transfer with the support and are stored therein, as above-mentioned.

There is a possibility that the H atoms formed via ordinary homolytic cleavage of H_2 on Pt could be directly added to the CAL molecules adsorbed on Pt. If the substrate molecules were adsorbed with their C=C and C=O bonds on Pt, the selectivity to COL would not be so high as observed (Tables 1 and 2) and the product distribution would be similar to that with the reference of Pt/TiO_2 catalyst (Table 2). The preferential adsorption of CAL with its C=O group on Pt is unlikely to occur on our Pt/TiH_2 catalyst similar to the reference Pt/TiO_2 one, for which no significant differences are seen in the size of Pt nanoparticles on the TiH_2 and TiO_2 supports reduced at 150 ºC. The present authors recently reported that for CAL hydrogenation over Zn-modified Pd particles, molecules of HCAL product were adsorbed with their C=O group and controlled the preferential adsorption of CAL molecules with their C=O group on the surface of metal particles.[19] As a result, the COL selectivity was observed to increase on the progress of reaction (accumulation of HCAL product). For the present CAL hydrogenation on Pt/TiH_2, the product distribution did not change during the reaction (Figure S1). In addition to these features, the value of H_2 pressure dependence of 1.18 (Figure 1) and the inclusion of D species of the support into the COL product (Table 3) indicate that the present CAL hydrogenation does not occur via ordinary hydrogenation processes with H· and the contribution of

hydrogenation on Pt surface is insignificant. The function of the surface of Pt nanoparticles on TiH_2 is to produce H (D) species by homolytic cleavage of gaseous H_2 (D_2) and to act as a source of H (D) species diffusing to the support. The reactivity of C=O of CAL substrate adsorbed at the TiH_2 - Pt particle boundary is high judging from its lower FTIR absorption frequency (Figure 6) and so the unique hydrogenation (ionic hydrogenation) should occur at a larger rate compared with the ordinary hydrogenation; the H species formed on Pt would be used preferentially for the compensation of hydrogen species in the TiH_2 support used for the ionic CAL hydrogenation.

The significant difference between H_2 and D_2 in the rate of CAL hydrogenation was observed when the catalyst was reduced in H_2 but not in D_2 (Table 3 and Table S3). The rate of CAL hydrogenation with D_2 is smaller than that with H_2 (isotope effect). This difference should result from the rate of diffusion of hydrogen species (H, D) into and within the support, which are formed on the surface of Pt crystallites. It is further demonstrated that the present CAL hydrogenation on Pt/TiH_2 catalyst takes place with H^+ and H^- from the support. For the Pt/TiH_2 reduced in H_2, which does not include D in the support, the diffusion of H may be faster/easier than that of D, according to the literature.[20] Smaller rate of D diffusion would be responsible for the

smaller rate of CAL hydrogenation in D_2. This indicates that the diffusion of hydrogen species within the TiH_2 support is a process determining the overall rate of hydrogenation. When the catalyst was reduced in D_2 ((1%Pt/TiH_2)-150D_2), some vacancy and interstitial sites of the support were occupied by D species and so the diffusion of D occurred faster than in the (1%Pt/TiH_2)-150H_2 when D_2 was the gas source. However, no isotope effect was observed on the high COL selectivity because the reaction processes should be the same irrespective of the reducing agents of H_2 and D_2.

Besides, the stability of the most active (1%Pt/TiH_2)-150H_2 was also tested. The deactivation of the catalyst was observed during the recycling runs, in which the conversion was 98%, 90%, and 57% for the first three runs, and the selectivity kept almost unchanged (about 97%). ICP results indicated about 26 w-% of the initial Pt loading was lost after the three test runs. Hence, the leaching of Pt is the main cause for the deactivation of catalyst. Some Pt species dissolved in the liquid phase might be active to the CAL hydrogenation (via homogeneous catalysis); however, this possibility should be unlikely because the high COL selectivity was obtained at any conversion level in one run and in repeated runs and the rate of CAL conversion was decreased during the recycling. That is, the present selective hydrogenation of CAL to

COL occurs heterogeneously on the surface of Pt/TiH_2 catalyst through several steps discussed above.

4. CONCLUSIONS

The unique Pt/TiH_2 catalyst that has hydrogen storage and release capability is effective for the selective hydrogenation of CAL to COL. A CAL molecule is preferentially adsorbed with its C=O group on Pt - TiH_2 boundary and this controlled CAL adsorption is favorable for its selective hydrogenation. The addition of two H atoms to the C=O group of CAL occurs by the attack of H^+ and H^- species from the support (ionic hydrogenation). The consumption of these hydrogen species of the support is compensated by gaseous H_2, which is dissociatively adsorbed on Pt and the H atoms formed change into H^+ and H^- via electron transfer during H spillover on and diffusion into the support. The change of 2H to H^+ and H^- takes place smoothly and so the direct addition of 2H to CAL (ordinary hydrogenation) is unlikely to occur. The unique structure of TiH_2 covered by a thin TiO_xH_y layer is helpful to separate and stabilize the H^+ and H^- species. The rate of CAL hydrogenation with Pt/TiH_2 reduced in H_2 depends on the gaseous dihydrogen used (H_2, D_2), in which the rate in D_2 is smaller than that in H_2 (isotope effect) and the diffusion rate of H and D species in the support is crucial.

ASSOCIATED CONTENT

Supporting Information

This material is available free of charge via the Internet at http://pubs.acs.org

Additional characterization results of XPS, TEM, XRD, CO chemisorption, Assignment of DRIFT absorption bands for COL on the catalysts, Time−Conversion/Selectivity profiles, TOF-H_2 pressure relationship, and Isotope effects at low conversion levels.

AUTHOR INFORMATION

Corresponding Authors

*E-mail: czhang@ciac.ac.cn

*E-mail: zhaofy@ciac.ac.cn

ORCID

Chao Zhang: 0000-0001-6669-1420

Fengyu Zhao: 0000-0001-6798-5287

ACKNOWLEDGEMENTS

We gratefully acknowledge the financial support provided by the National Natural Science Foundation of China (21872134, 21473179), National Program on Key Research Project (2016YFA0602900), International Cooperation Project of Jilin Province (20170414012GH), the Youth Innovation Promotion Association (2014203), and CAS President's International Fellowship Initiative（PIFI）2018CV0012, Chinese Academy of Science.

REFERENCES

1. (A) Wang, L.; Guan, E.; Zhang, J.; Gates, B. C.; Xiao, F. S., Single-Site Catalyst Promoters Accelerate Metal-Catalyzed Nitroarene Hydrogenation. *Nat. Commun.* **2018,** *9*, 1362; (B) Bullock, R. M., Abundant Metals Give Precious Hydrogenation Performance. *Science* **2013,** *342*, 1054-1055; (C) Bai, S.; Bu, L.; Shao, Q.; Zhu, X.; Huang, X., Multicomponent Pt-Based Zigzag Nanowires as Selectivity Controllers for Selective Hydrogenation Reactions. *J. Am. Chem. Soc.* **2018,** *140*, 8384-8387; (D) Kennedy, G.; Baker, L. R.; Somorjai, G. A., Selective Amplification of C=O Bond Hydrogenation on Pt/TiO_2: Catalytic Reaction and Sum-Frequency Generation Vibrational Spectroscopy Studies of Crotonaldehyde Hydrogenation. *Angew. Chem. Int. Ed.* **2014,** *53*, 3405-3408; (e) Stephan, D. W., A Metal-Free Landmark. *Nat. Chem.* **2014,** *6*, 952; (f) Ryabchuk, P.; Agostini, G.; Pohl, M. M.; Junge, K.; Beller,

M., Intermetallic Nickel Silicide Nanocatalyst−A Non-Noble Metal–Based General Hydrogenation Catalyst. *Sci. Adv.* **2018,** *4*, eaat0761; (g) Zhao, M.; Yuan, K.; Li, G.; Zhao, H.; Tang, Z., Metal–Organic Frameworks as Selectivity Regulators for Hydrogenation Reactions. *Nature* **2016,** *539*, 76; (h) Huang, F.; Deng, Y.; Chen, Y.; Cai, X.; Peng, M.; Jia, Z.; Ren, P.; Xiao, D.; Wen, X.; Wang, N.; Liu, H.; Ma, D., Atomically Dispersed Pd on Nanodiamond/Graphene Hybrid for Selective Hydrogenation of Acetylene. *J. Am. Chem. Soc.* **2018,** *140*, 13142-13146; (i) Niu, W.; Gao, Y.; Zhang, W.; Yan, N.; Lu, X., Pd–Pb Alloy Nanocrystals with Tailored Composition for Semihydrogenation: Taking Advantage of Catalyst Poisoning. *Angew. Chem. Int. Ed.* **2015,** *54*, 8271-8274; (j) Baker, L. R.; Kennedy, G.; Spronsen, V. M.; Hervier, A.; Cai, X.; Chen, S.; Wang, L. W.; Somorjai, G. A., Furfuraldehyde Hydrogenation on Titanium Oxide-Supported Platinum Nanoparticles Studied by Sum Frequency Generation Vibrational Spectroscopy: Acid-Base Catalysis Explains the Molecular Origin of Strong Metal-Support Interactions. *J. Am. Chem. Soc.* **2012,** *134*, 14208-14216; (k) Ren, D.; He, L.; Yu, L.; Ding, R. S.; Liu, Y. M.; Cao, Y.; He, H. Y.; Fan, K. N., An Unusual Chemoselective Hydrogenation of Quinoline Compounds Using Supported Gold Catalysts. *J. Am. Chem. Soc.* **2012,** *134*, 17592-17598.

2. Lu, Y.; Yamamoto, Y.; Almansour, A. I.; Kumar, R. S.; Bao, M., Unsupported Nanoporous Palladium-Catalyzed Chemoselective Hydrogenation of Quinolines: Heterolytic Cleavage of H_2 Molecule. *Chin. J. Catal.* **2018,** *39*, 1746-1752.

3. (a) Tamura, M.; Tokonami, K.; Nakagawa, Y.; Tomishige, K., Selective Hydrogenation of Crotonaldehyde to Crotyl Alcohol over Metal Oxide Modified Ir Catalysts and Mechanistic Insight. *ACS Catal.* **2016,** *6*, 3600-3609; (b) Skara, G.; Vleeschouwer, D. F.; Geerlings, P.; Proft, D. F.; Pinter, B., Heterolytic Splitting of Molecular Hydrogen by Frustrated and Classical Lewis Pairs: A Unified Reactivity Concept. *Sci. Rep.* **2017,** *7*, 16024; (c) Shimizu, K.; Miyamoto, Y.; Satsuma, A., Size- and Support-Dependent Silver Cluster Catalysis for Chemoselective Hydrogenation of Nitroaromatics. *J. Catal.* **2010,** *270*, 86-94; (d) Fiorio, J. L.; López, N.; Rossi, L. M., Gold–Ligand-Catalyzed Selective Hydrogenation of Alkynes into Cis-Alkenes via H_2 Heterolytic Activation by Frustrated Lewis Pairs. *ACS Catal.* **2017,** *7*, 2973-2980; (e) Fiorio, J. L.; Gonçalves, R. V.; Teixeira-Neto, E.; López, N.; Rossi, L. M., Accessing Frustrated Lewis Pair Chemistry Through Robust Gold@N-Doped Carbon for Selective Hydrogenation of Alkynes. *ACS Catal.* **2018,** *8*, 3516-3524.

4. (a) Stephan, D. W., The Broadening Reach of Frustrated Lewis Pair Chemistry. *Science* **2016,** *354*, aaf7229; (b) Welch, G. C.; Juan, R. R. S.; Masuda, J. D.; Stephan,

D. W., Reversible, Metal-Free Hydrogen Activation. *Science* **2006,** *314*, 1124-1126; (c) Zhang, S.; Huang, Z. Q.; Ma, Y.; Chang, C. R.; Qu, Y., Solid Frustrated-Lewis-Pair Catalysts Constructed by Regulations on Surface Defects of Porous Nanorods of CeO_2. *Nat. Commun.* **2017,** *8*, 15266; (d) Ullrich, M.; Lough, A. J.; Stephan, D. W., Reversible, Metal-Free, Heterolytic Activation of H_2 at Room Temperature. *J. Am. Chem. Soc.* **2009,** *131*, 52-53; (e) Chernichenko, K.; Madarász, Á.; Pápai, I.; Nieger, M.; Leskelä, M.; Repo, T., A Frustrated Lewis Pair Approach to Catalytic Reduction of Alkynes to Cis-Alkenes. *Nat. Chem.* **2013,** *5*, 718.

5. Maj, L.; Grochala, W., Theoretical Design of Catalysts for the Heterolytic Splitting of H_2. *Adv. Funct. Mater.* **2006,** *16*, 2061-2076.

6. (a) Hu, G.; Wu, Z.; Jiang, D., First Principles Insight into H_2 Activation and Hydride Species on TiO_2 Surfaces. *J. Phys. Chem. C* **2018,** *122*, 20323-20328; (b) Ghuman, K. K.; Wood, T. E.; Hoch, L. B.; Ozin, G. A.; Singh, C. V., Illuminating CO_2 Reduction on Frustrated Lewis Pair Surfaces: Investigating the Role of Surface Hydroxides and Oxygen Vacancies on Nanocrystalline $In_2O_{3-x}(OH)_y$. *Phys. Chem. Chem. Phys.* **2015,** *17*, 14623-14635; (c) Tamura, M.; Yonezawa, D.; Oshino, T.; Nakagawa, Y.; Tomishige, K., In Situ Formed Fe Cation Modified Ir/MgO Catalyst for Selective Hydrogenation of Unsaturated Carbonyl Compounds. *ACS Catal.* **2017,**

7, 5103-5111; (d) Tamura, M.; Tokonami, K.; Nakagawa, Y.; Tomishige, K., Effective NbO_x-Modified Ir/SiO_2 Catalyst for Selective Gas-Phase Hydrogenation of Crotonaldehyde to Crotyl Alcohol. *ACS Sust. Chem. Eng.* **2017,** *5*, 3685-3697.

7. (a) El-Eskandarany, M. S.; Shaban, E.; Aldakheel, F.; Alkandary, A.; Behbehani, M.; Al-Saidi, M., Synthetic Nanocomposite MgH_2/5 Wt.% $TiMn_2$ Powders for Solid-Hydrogen Storage Tank Integrated with PEM Fuel Cell. *Sci. Rep.* **2017,** *7*, 13296; (b) Reilly, J., J., ; Stephan, D. W., Hydrogen Storage in Metal Hydrides. *Sci. Am.* **1980,** *242*, 118 - 129; (c) P. M. S., Jones; P., Ellis; T., Aslett, Thermal Stability of Metal Hydrides, Deuterides and Tritides. *Nature* **1969,** *223*, 829.

8. (a) Wu, Q. F.; Zhang, C.; Zhao, F. Y., Highly Selective Pt/Ordered Mesoporous TiO_2–SiO_2 Catalysts for Hydrogenation of Cinnamaldehyde: the Promoting Role of Ti^{2+}. *J. Colloid Interf. Sci.* **2016,** *463*, 75-82; (b) Fu, Q.; Wagner, T., Interaction of Nanostructured Metal Overlayers with Oxide Surfaces. *Surf. Sci. Rep.* **2007,** *62*, 431-498; (c) Kim, M. S.; Chung, S. H.; Lee, K. Y., Catalytic Reduction of Nitrate in Water over Pd–Cu/TiO_2 Catalyst: Effect of the Strong Metal-Support Interaction (SMSI) on the Catalytic Activity. *Appl. Catal. B: Environ.* **2013,** *142-143*, 354-361.

9. Takeda, Y.; Tamura, M.; Nakagawa, Y.; Okumura, K.; Tomishige, K., Hydrogenation of Dicarboxylic Acids to Diols over Re–Pd Catalysts. *Catal. Sci. Technol.* **2016,** *6*, 5668-5683.

10. Koso, S.; Nakagawa, Y.; Tomishige, K., Mechanism of the Hydrogenolysis of Ethers over Silica-Supported Rhodium Catalyst Modified with Rhenium Oxide. *J. Catal.* **2011,** *280* (2), 221-229.

11. (a) Mandrino, D.; Paulin, I.; Škapin, S. D., Scanning electron microscopy, X-Ray Diffraction and Thermal Analysis Study of the TiH_2 Foaming Agent. *Mater. Charact.* **2012,** *72*, 87-93; (b) Ma, M.; Liang, L.; Wang, L.; Xiang, W.; Tan, X., Phase Transformations of Titanium Hydride in Thermal Desorption Process with Different Heating Rates. *Int. J. Hydrogen Energy* **2015,** *40*, 8926-8934; (c) Wang, C.; Zhang, Y.; Wei, Y.; Xiao, S.; Chen, Y., XPS Study of the Deoxidization Behavior of Hydrogen in TiH_2 Powders. *Powder Technol.* **2016,** *302*, 423-425.

12. Mingwang, M.; Lei, W.; Yuan, W.; Wei, X.; Ping, L.; Binghua, T.; Xiaohua, T., Effect of Hydrogen Content on Hydrogen Desorption Kinetics of Titanium Hydride. *J. Alloys Compd.* **2017,** *709*, 445-452.

13. (a) Zhang, Y.; Zhuang, X.; Zhu, Y.; Li, L.; Dong, J., Synergistic Effects of TiH_2 and Pd on Hydrogen Desorption Performances of MgH_2. *Int. J. Hydrogen Energy* **2015,** *40*, 16338-16346; (b) Sakintuna, B.; Lamari Darkrim, F.; Hirscher, M., Metal Hydride Materials for Solid Hydrogen Storage: A Review. *Int. J. Hydrogen Energy* **2007,** *32*, 1121-1140.

14. (a) Paulin, I.; Donik, Č.; Mandrino, D.; Vončina, M.; Jenko, M., Surface Characterization of Titanium Hydride Powder. *Vacuum* **2012,** *86*, 608-613; (b) Zhang, Y.; Wang, C.; Liu, Y.; Xiao, S.; Chen, Y., Surface Characterizations of TiH_2 Powders Before and After Dehydrogenation. *Appl. Surf. Sci.* **2017,** *410*, 177-185.

15. Kennedy, A. R.; Lopez, V. H., The Decomposition Behavior of As-Received and Oxidized TiH_2 Foaming-Agent Powder. *Mater. Sci. Eng. : A* **2003,** *357*, 258-263.

16. (a) Rokhmanenkov, A. S.; Kuksin, A. Y.; Yanilkin, A. V., Simulation of Hydrogen Diffusion in $TiH_{(x)}$ Structures. *Phys. Met. Metallography* **2017,** *118*, 28-38; (b) Park, M. S.; Janotti, A.; Van de Walle, C. G., Formation and Migration of Charged Native Point Defects in MgH_2: First-Principles Calculations. *Phys. Rev. B* **2009,** *80*, 064102.

17. Prins, R., Hydrogen Spillover Facts and Fiction. *Chem. Rev.* **2012,** *112*, 2714-2738.

18. Novoselov, II; Yanilkin, A. V., Hydrogen Diffusion in Titanium Dihydrides from First Principles. *Acta Materialia* **2018,** *153*, 250-256.

19. Fujita, S.; Mitani, H.; Zhang, C.; Li, K.; Zhao, F.; Arai, M., Pd and PdZn Supported on ZnO as Catalysts for the Hydrogenation of Cinnamaldehyde to Hydrocinnamyl Alcohol. *Mol. Catal.* **2017,** *442*, 12-19.

20. Wipf, H.; Kappesser, B.; Werner, R., Hydrogen Diffusion in Titanium and Zirconium Hydrides. *J. Alloys Compd.* **2000,** *310*, 190-195.

TOC